GEOPHYSICAL RESEARCH LETTERS, VOL. 28, NO. 18, PAGES 3497-3500, SEPTEMBER 15, 2001

An edge detection technique to estimate melt duration, season and melt extent on the Greenland ice sheet using passive microwave data

Maneesha Joshi[1,2], Carolyn J. Merry [3], Kenneth C. Jezek[4] and John F. Bolzan[4]

Abstract. The melt extent, duration and melt season on the Greenland ice sheet were estimated using an edge detection technique on passive microwave data from the SSM/I and SMMR instruments (18/19V GHz channel) for the period 1979 to 1997. The annual brightness temperature (Tb) time series at a pixel location that experiences summer melt has a steep rise and drop in Tb with the onset and end of melt, respectively. A derivative-of-Gaussian edge detector is used to detect edges corresponding to the onset and end of melt. The time lapsed between the first upward and last downward edge on the annual Tb time series gives an estimate of the melt season and the time lapsed between successive upward and downward edges gives the duration of melt. While the maximum melt extent increased by 18%, the total duration of melt increased by 3.7% and the total melt season decreased by 3.8% during the period 1979-1997.

Introduction

There is an increasing interest in climate change issues among scientists and the general public. Current scientific consensus supports polar amplification of global warming [*Barron*, 1995] and there is, therefore, a need to efficiently monitor and understand the mass balance and physical properties of the polar ice sheets. The Greenland ice sheet loses mass from the calving of icebergs and melt runoff in summer [*Pfeffer, et al.*, 1991]. Coastal and southern regions of the Greenland ice sheet experience melt in summer and some of the meltwater from the ice sheet margin runs off the ice sheet while the rest refreezes within the snowpack. An understanding of the formation of meltwater on the ice sheet, together with direct measurements of change in the ice sheet mass, could enable better prediction of the ice sheet response to future climate forcings [*Krabill, et al.*, 2000].

Spaceborne remote sensing is well suited to measuring physical properties of the Greenland ice sheet. Microwave sensors in particular are applicable because of their large spatial coverage and all weather, day-night observations. Moreover, passive microwave data for the Greenland ice sheet are available since 1979 and the collection of such data is ongoing. Long term monitoring of the Greenland ice sheet is, therefore, possible with satellite passive microwave data. Data from the Scanning Multichannel Microwave Radiometer (SMMR) and the Special Sensor Microwave / Imager (SSM/I) in the 18/19V GHz channels that were used in this study were obtained from the National Snow and Ice Data Center (NSIDC) at Boulder, Colorado.

Surface melt on the Greenland ice sheet has previously been estimated from passive microwave data using melt thresholds for the cross-polarized gradient ratio [*Abdalati and Steffen*, 1997] and gradient ratio [*Abdalati and Steffen*, 1995], and using the 37 GHz channel with a radiative transfer model to arrive at a melt threshold [*Mote and Anderson*, 1995]. This study uses synthetic aperture radar (SAR) data to select passive microwave signature pixels from melt regions (percolation and other melt facies) and areas that remain dry. The specific melt signature consists of an abrupt change in brightness temperature (Tb) associated with the first appearance (or disappearance) of a few percent by volume of free water in the surface snow [*Garrity*, 1992]. The annual brightness temperature time series of the signature pixels was used to select a suitable edge detector and threshold that detects these abrupt changes in Tb as edges. The 18/19V GHz frequency channel was used in this study because it has the largest mean difference in Tb between melt and non-melt seasons and shows a lower fluctuation in Tb within a season [*Mote, et al.*, 1993]. This made the selection of the edge detector easier and the detection of edges more robust.

Methodology

Wet areas (made up of the percolation, wet and bare ice snow facies) can be distinguished from the dry areas on the Greenland SAR mosaic based on relative intensity [*Fahnestock, et al.*, 1993]. Twenty-six wet and dry pixels were chosen from their representative areas based on the Greenland SAR mosaic. An edge detector and a threshold that would detect edges in the Tb time series for wet signature pixels, but none for the dry signature pixels were used. Several edge filters including a Sobel filter and a Laplacian of Gaussian were tested. By a trial and error process, a 17-point derivative of Gaussian edge detector with $\sigma = 2$, which combines smoothing and edge detection, with a threshold of $\pm$ 6.4 was selected for the entire time period. A sensitivity analysis of the size and σ of the derivative of Gaussian edge detector showed no change in the trends concluded in this study.

The convolution of the annual Tb time series for a typical wet pixel with the derivative of Gaussian filter is shown in Figure 1a. The Tb time series for the wet pixel is labeled 'wet pixel Tb' and shown for reference (the scale is different

[1]DEAS, Harvard University, Cambridge, Massachusetts.
[3]Dept. of Civil & Environmental Eng. and Geodetic Sci., Ohio State University, Columbus, Ohio.
[4]Byrd Polar Research Center, Ohio State University, Columbus, Ohio.
[2]Now at GDT, 11 Lafayette St., Lebanon, New Hampshire.

Paper number 2000GL012503.
0094-8276/01/2000GL012503$05.00

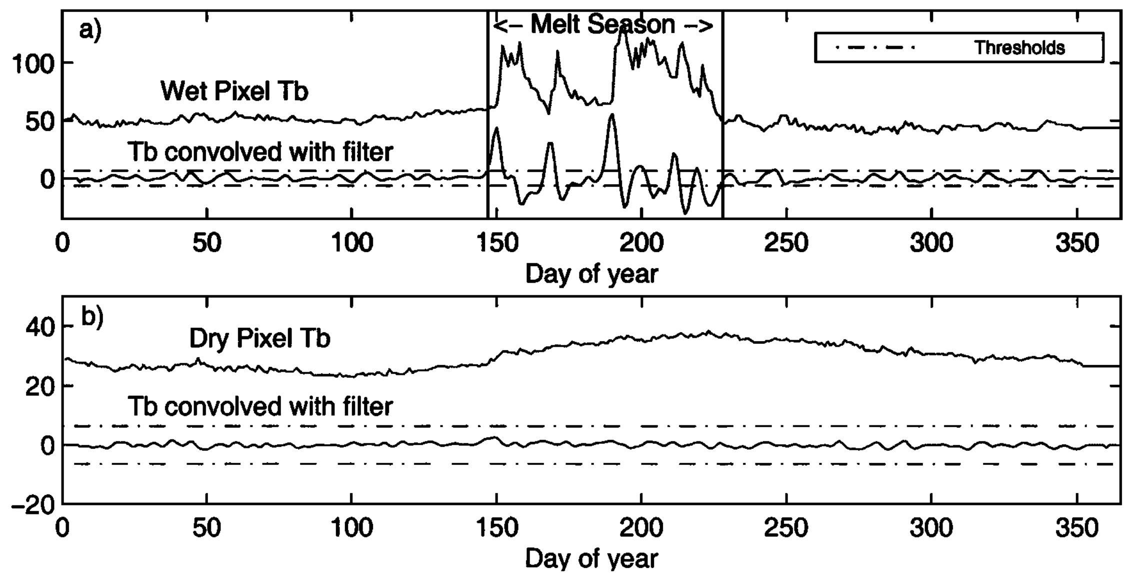

Figure 1. Edge detection on the annual Tb (19V GHz) time series for a typical a) wet pixel and b) dry pixel. The start and end of melt are detected on day 147 and 228, respectively, in a). There are no edges detected for the dry pixel.

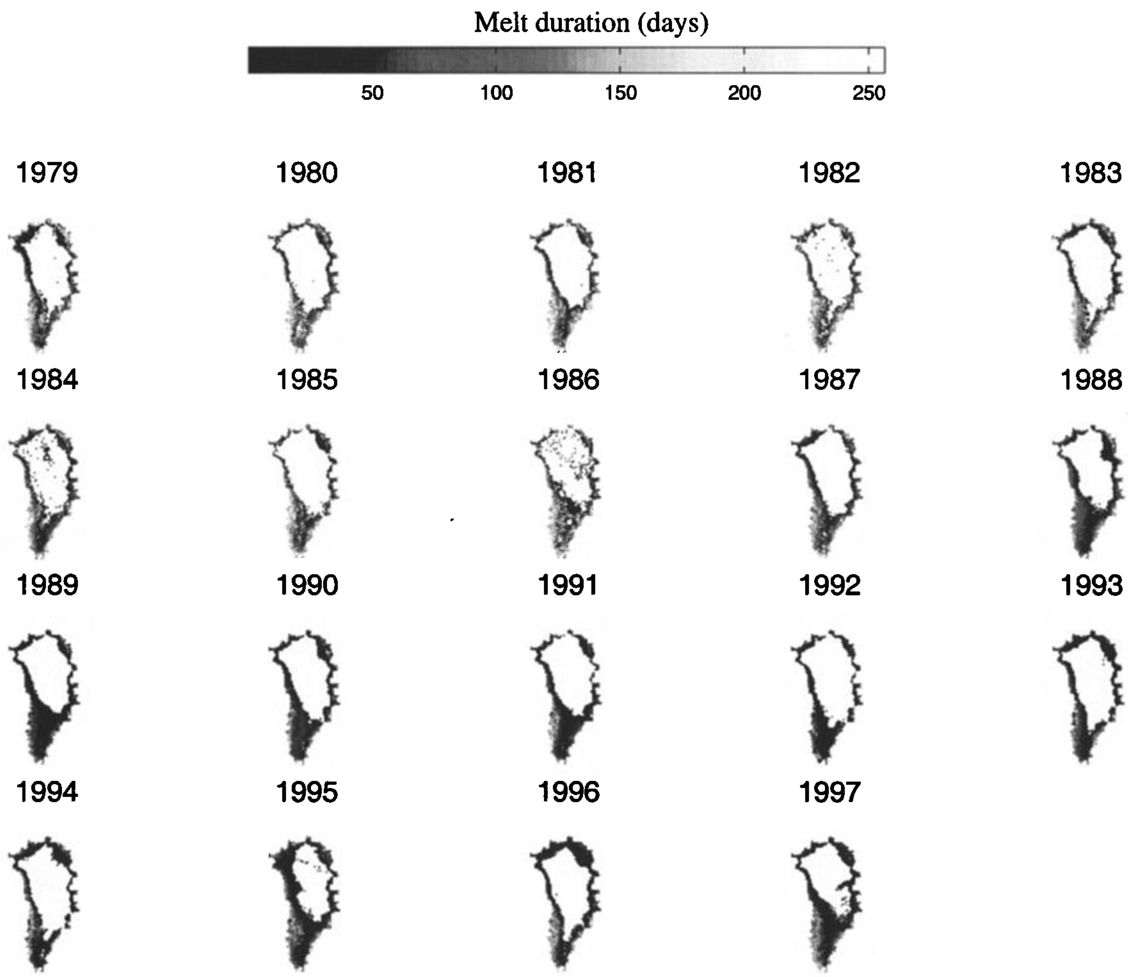

Figure 2. Total duration of melt on the Greenland ice sheet for the years 1979-1997.

and is not indicated). A threshold of 6.4 for upward and -6.4 for downward edges was used. The first upward edge indicating the start of melt was detected on day 147 and the last downward edge indicating the end of melt occurred on day 228, giving a melt season of 81 days. The actual melt duration, which is the sum of days between successive upward and downward edges, was 77. The convolution of the edge filter with a typical dry pixel Tb time series (Figure 1b) showed no threshold crossings.

This edge detection technique was applied to all the ice sheet pixels (land pixels were masked out) for all years of passive microwave data (1979 - 1997). The SMMR data were calibrated with the SSM/I data using the cross calibration coefficients for Antarctica [*Jezek, et al.*, 1993].

Results and Discussion

The melt areas on the Greenland ice sheet for the years 1979 through 1997 are shown in Figure 2. The white interior regions of the ice sheet are the dry snow areas. The melt areas are shaded according to their melt duration (not melt season), with a darker shade indicating a shorter duration of melt. For a pixel, the melt season is defined as the time between the first upward and last downward edge. The duration of melt at a pixel location is the total time of melt events computed as the sum of times lapsed between successive upward and downward edges.

In general, melt is observed along low-elevation coastal regions and on the southern parts of the ice sheet. Areas adjoining the dry snow region are the darkest, indicating they have the shortest duration of melt, as would be expected. As one moves away from the interior, however, the duration of melt increases as indicated by the lighter shade. In 1992, a short melt duration, in addition to a larger dry snow area, is seen and the cooler conditions in the southern regions seem to persist into 1994.

The annual maximum melt extent for the period 1979-1997 is shown in Figure 3. The annual maximum melt extent includes all pixels that exhibit a melt signature (the detection of an edge) during a year. A slight drop in maximum melt extent in the early 1980's was followed by an overall increase in maximum melt extent, which was punctuated by a sharp drop in the early 1990's due to cooling following the eruption of Mt. Pinatubo in 1991. Since 1992 there appears to be a marked increase in maximum melt extent.

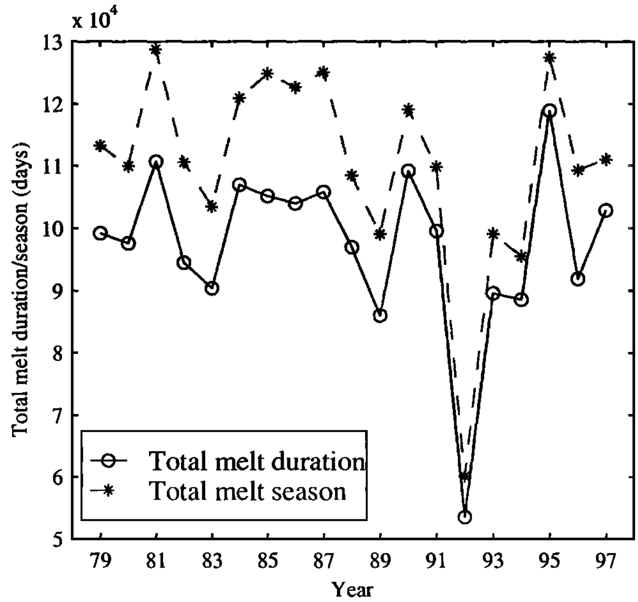

Figure 4. Total melt duration and season on the Greenland ice sheet for 1979-1997.

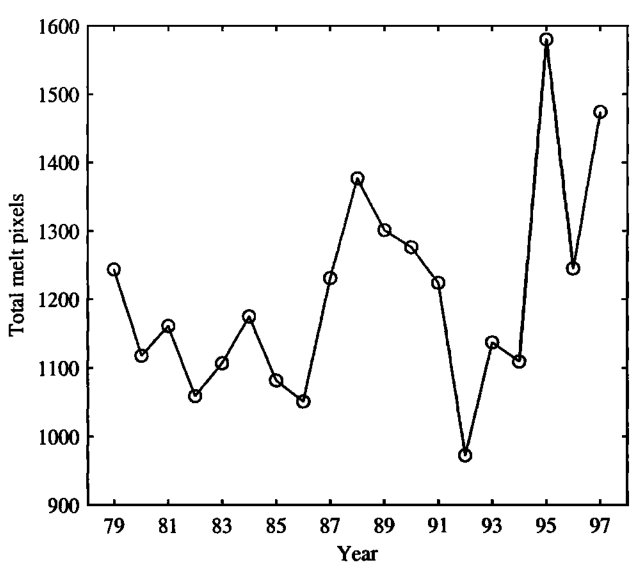

Figure 3. Maximum melt extent on the Greenland ice sheet for 1979-1997.

The annual total melt duration was calculated as the cumulative sum of melt duration (in days) of all the pixels that experienced melt in a year. The total melt season was computed by summing the melt season for each pixel experiencing melt. The variation in total melt season and total melt duration for the years 1979-1997 is plotted in Figure 4. The total duration is less than the total melt season because there are days without any melt in the summer melt season.

The total melt season and duration trend is not strongly correlated with the maximum melt extent trend. The correlation coefficient between the maximum melt extent and total melt duration was 0.52 and that between melt extent and total melt season was only 0.38. The melt extent trends and the melt season/duration trends need not be similar. For example, a short and very warm summer can produce a large maximum areal extent of melt but a short melt season/duration, and conversely, a long summer with no unusual warm event may show normal maximum melt extent with a higher than average total melt season /duration. Variations in the annual maximum melt extent are primarily caused by changes in melt along the dry/melt area boundary and typically these boundary pixels have short melt durations. Thus, changes in the maximum melt extent may not affect the overall melt season or duration significantly. For example, in the present analysis, the maximum melt extent in 1989 was more than that in 1990 (Figure 3), but the total melt season/duration for 1990 was more than that in 1989 (Figure 4).

Previous studies related to surface melt on the Greenland ice sheet have estimated a 3.8% annual increase in the mean daily melt extent (May-August) [*Mote and Anderson*, 1995] and a 4.4% annual increase in the mean monthly (June-August) melt extent from 1979 to 1991 [*Abdalati and

Steffen, 1997]. Although the annual maximum melt extent and the total melt duration/season based on the edge technique show little change for the period 1979-1991, qualitatively, the trends observed here are similar to those previously reported. These include the increasing trend in maximum melt extent in the late 1980's and the sharp drop in maximum melt extent in 1992. For the 19 year period (1979-1997), the maximum melt extent increased by 18% of 1979 values, while the total melt duration increased by 3.7% and the total melt season decreased by 3.8% of 1979 values. These results are significant given the observation that changes in maximum melt extent need not be associated by a corresponding change in melt season and duration. The edge detection technique provides estimates of not only melt extent, but also melt season and duration, which can be used to better understand the sensitivity of melt on the ice sheet to climatic changes.

Conclusions

The edge detection technique was used to estimate the maximum melt extent, the duration of melt and melt season on the Greenland ice sheet using passive microwave data for the period 1979-1997. This study finds an increasing trend in melt extent for the study period, but no corresponding increase (of same magnitude) in the total melt season or duration. This is because changes in maximum melt extent are primarily caused by pixels along the melt / dry boundary, which have short melt durations that may not affect the total melt season/duration. By combining the melt extent information with melt duration one can begin to measure sensitivities in the melt process associated with variability in the surface heat budget. As a step in that direction, these results have further been used to determine absorbed shortwave flux on the ice sheet by using an albedo scheme based on the melt season estimated by the edge detection method [*Joshi*, 1999].

References

Abdalati, W., and K. Steffen, Passive microwave-derived snow melt regions on the Greenland ice sheet, *Geophys. Res. Lett., 22,* 787-790, 1995.

Abdalati, W., and K. Steffen, Snowmelt on the Greenland ice sheet as derived from passive microwave satellite data, *Journal of Climate, 10,* 165-175, 1997.

Barron, E. J., Global change researchers assess projections of climate change, *EOS, 78(18),* 185-190, 1995.

Fahnestock, M. A., R. Bindschadler, R. Kwok, and K. C. Jezek, Greenland ice sheet surface properties and ice dynamics from ERS-1 SAR imagery, *Science, 262(5139),* 1530-1534, 1993.

Garrity, C., Characterization of snow on floating ice and case studies of brightness temperature changes during onset on melt, in F. D. Carsey (ed.), *Microwave remote sensing of sea ice,* Geophysical Monograph 68, AGU, 1992.

Jezek, K. C., C. J. Merry, and D. Cavalieri, Comparison of SMMR and SSM/I passive microwave data collected over Antarctica, *Annals of Glaciology, 17,* 131-136, 1993.

Joshi, M. D., Estimation of surface melt and absorbed radiation on the Greenland ice sheet using passive microwave data, *PhD Dissertation,* Ohio State University, 1999.

Krabill, W., W. Abdalati, E. Frederick, S. Manizade, C. Martin, J. Sonntag, R. Swift, R. Thomas, W. Wright, and J. Yungel, Greenland Ice Sheet: High-elevation balance and peripheral thinning, *Science, 289(5478),* 428-430, 2000.

Mote, T. L., and M. R. Anderson, Variations in snowpack melt on the Greenland ice sheet based on passive microwave measurements, *Journal of Glaciology, 41,* 51-60, 1995.

Mote, T. L., M. R. Anderson, K. C. Kuivinen and C. M. Rowe, Passive microwave-derived spatial and temporal variations of summer melt on the Greenland ice sheet, *Annals of Glaciology, 17,* 233-238, 1993.

Pfeffer, W.T., M. F. Meier, and T. H. Illangasekare, Retention of Greenland runoff by refreezing: Implications for projected future sea-level change,*Journal of Geophysical Research, 96(C-12):22,* 117-124, 1991.

M. Joshi, Geographic Data Technology, 11 Lafayette St, Lebanon, NH 03766. (e-mail: maneesha_joshi@gdt1.com)

C. J. Merry, Dept. of Civil and Environmental Eng. and Geodetic Science, The Ohio State University, Columbus, OH 43210. (e-mail: merry.1@osu.edu)

K. C. Jezek and J. F. Bolzan, Byrd Polar Research Center, 1090 Carmack Road, The Ohio State University, Columbus, OH 43210. (e-mail: jezek@iceberg.mps.ohio-state.edu; bolzan.1@osu.edu)

(Received October 18, 2000; accepted May 21, 2001